NASA TN D-1408

TECHNICAL NOTE

D-1408

VAPORIZATION RATES OF ETHANOL SPRAYS IN A COMBUSTOR WITH LOW-FREQUENCY FLUCTUATIONS OF COMBUSTION-GAS PRESSURE

By Robert D. Ingebo

Lewis Research Center
Cleveland, Ohio

NATIONAL AERONAUTICS AND SPACE ADMINISTRATION

WASHINGTON

October 1962

NATIONAL AERONAUTICS AND SPACE ADMINISTRATION

TECHNICAL NOTE D-1408

VAPORIZATION RATES OF ETHANOL SPRAYS IN A COMBUSTOR WITH LOW-FREQUENCY FLUCTUATIONS OF COMBUSTION-GAS PRESSURE

By Robert D. Ingebo

SUMMARY

Experimental heat-transfer and drag coefficients were obtained for ethanol drops burning in the presence of low-frequency chamber-pressure fluctuations of predominant frequencies of 90 to 100 cps. These coefficients were within ±10 percent of values determined from transfer relations obtained previously for relatively steady combustion in rocket combustors. Also, the theoretically predicted effect of completeness of fuel-spray vaporization on combustor performance was compared with experimental results. The percent by volume of the total fuel vaporized was within ±2 percent of the square of the characteristic-exhaust-velocity efficiency of the combustor.

INTRODUCTION

Knowledge of the rates of exchange of heat, mass, and momentum within combustion chambers is needed to determine relations existing between the acceleration of combustion-gas streams and the vaporization rates of fuel sprays accelerating and burning in the combustor. In reference 1, heat-transfer and drag coefficients were determined for ethanol drops burning in a relatively stable combustion environment. Such information has proved useful for predicting the combustion performance of rockets (ref. 2). The combustion of liquid propellants in rocket engines, however, is often accompanied by pressure fluctuations in the combustion chamber as well as in the propellant injection system. Similar heat-transfer- and drag-coefficient data for drops burning in the presence of combustion oscillations are therefore needed to obtain a more general understanding of the combustion process.

This investigation was made to determine the effect of an environment of low-frequency combustion oscillations on the vaporization of ethanol drops burning in a rocket chamber. Drop-size distribution and

drop-velocity data were obtained for ethanol sprays burning in the presence of low-frequency fluctuations of gas pressure by photographing the spray in a low-thrust rocket combustor with a high-speed camera developed at the Lewis Center (ref. 3). Thus, from these data and from combustion-gas-velocity data, it was possible to calculate heat-transfer and drag coefficients, which were compared with the values obtained for steady-state combustion (ref. 1).

RESULTS AND DISCUSSION

Experimental Investigation

The rocket combustor, high-speed camera, and auxiliary equipment that were used in this investigation are shown in figure 1. A description of the development of the photographic technique and the procedure for operating the combustor are given in reference 3. With this equipment, it was possible to obtain size-distribution data for drops burning in a combustion chamber.

In order to vary the fineness of atomization, an injector was used, as shown in detail in figure 2. Ethanol (95 percent ethanol and 5 percent water) was injected into the rocket chamber through the center tube. A pair of nitrogen-gas jets was impinged upon the fuel jet at an angle of 45° and at a distance of 1 inch from the fuel orifice in the injector face. Using a nitrogen-gas flow rate of 0.027 pound per second produced a relatively fine spray. For the second set of test conditions, a coarse spray was produced with a nitrogen-gas flow rate of only 0.002 pound per second. Liquid oxygen was injected into the rocket chamber through the two parallel rows of orifices in the face of the injector shown in figure 2. Also, a nitrogen-gas flow rate of 0.07 pound per second was used for internal cooling of the combustor windows shown in figure 1.

Traces of chamber-pressure variation with time during the rocket-firing test (fig. 3) were obtained with a strain-gage pressure transducer and a direct-writing oscillograph for two atomization conditions. Relatively low-frequency pressure fluctuations were observed in both cases. The amplitudes of the oscillations as well as the time-averaged chamber pressure, however, were considerably greater for combustion of the finer spray. By means of a tape recorder and frequency analyzer, the data shown in figure 4 were obtained to determine the frequency spectrum of the chamber-pressure fluctuations. The frequencies ranged from 50 to 200 cps and peaked at approximately 100 cps for the fine spray and approximately 90 cps for the coarse spray. Values of $\Delta P_c/P_c$ were approximately 37 percent for the fine spray and 10 percent for the coarse spray (fig. 3). (All symbols are defined in appendix A.)

The chamber-pressure fluctuations were considerably below the longitudinal acoustic frequency of the combustion chamber, which was approximately 1200 cps. Also, they could not be attributed to combustion-gas residence time (approximately 2 msec). The fluctuations of the chamber pressure, however, were reproducible and, therefore, useful to this investigation even though their source was not determined.

Photomicrographs of the fuel spray were obtained at camera stations 6, 10, and 15 inches downstream from the injector. The photomicrograph shown in figure 5 was taken at the 10-inch station. Droplet images magnified 14 times actual size were obtained with the aforementioned camera lens system. Drop diameters were measured directly from contact prints with an eyepiece having small scale subdivisions of 0.10 millimeter and thus were accurate to within ±7 microns. Only drop images that were in sharp focus were measured. Table I shows the drop-size-distribution data obtained for combustion of relatively fine and coarse sprays at distances of 6, 10, and 15 inches downstream from the injector face. Approximately 40 photomicrographs were used to compute each set of drop-size data.

Drop-velocity data were obtained with an accuracy of ±15 feet per second with a high-speed rotating mirror incorporated in the camera unit to track the burning drops and to stop their images on the $9\frac{1}{2}$-inch-wide infrared film. Since large drops moved at relatively low velocities as compared with the high velocity of small drops, a low mirror speed was required for them. Several pictures over a range of mirror speeds were thus needed to obtain the average velocity for a given-size drop at a particular downstream distance. The drop-velocity data (fig. 6) are average values obtained from at least 40 photomicrographs. Only one photomicrograph was obtained for each test firing of the rocket.

Average values of combustion-gas velocity were obtained from four runs at each station (fig. 7) with a streak-type 16-millimeter camera (100-ft/sec film speed). This camera was used to photograph the flame through a combustor window with a 1/8- by 1-inch slit located in the same plane as, but at an angle of 90° to, the windows used for the high-speed tracking camera. Random variations of ±10 percent in the combustion-gas velocity were observed for conditions of high-amplitude chamber-pressure fluctuations.

Heat-Transfer Relations

The rate of heat transfer dQ/dt to a single drop of fuel vaporizing and burning in a high-velocity and high-temperature combustion-gas stream may be expressed as

$$\frac{dQ}{dt} = H_T \frac{dm}{dt} = \pi D k_g \Delta T \, Nu \qquad (1)$$

where H_T is the total heat gained by an incremental weight of liquid dm. In a three-step process prior to actual combustion, the incremental weight dm gains sensible heat when the liquid is heated from the injection temperature T_l to the boiling point T_s. The liquid is then vaporized by gaining the required heat of vaporization H_v; finally, the vapor gains sensible heat in being heated to the temperature T_y. Thus,

$$H_T = H_v + c_{p,l}(T_s - T_l) + c_{p,v}(T_y - T_s) \tag{2}$$

and the Nusselt number Nu in equation (1) is thus evaluated at the temperature T_y.

Equation (1) may be rewritten in terms of the rate of droplet-area change as follows:

$$\frac{dA}{dt} = \pi\lambda Nu \tag{3}$$

where $\lambda = 4k_g \Delta T/\rho_l H_T$. In order to apply equation (3) to a spray of drops, it may be rewritten as

$$\frac{dA_T}{dt} = \frac{\pi\, d\left(\sum_{D=0}^{D=D_m} nD^2\right)}{dt} = \pi\lambda\overline{Nu} \sum_{D=0}^{D=D_m} n \tag{4}$$

Since

$$\sum_{D=0}^{D=D_m} nD^2 = N_T D_{20}^2$$

and

$$\sum_{D=0}^{D=D_m} n = N_T$$

equation (4) becomes

$$\frac{d\left(N_T D_{20}^2\right)}{dt} = \lambda N_T \overline{Nu} \tag{5}$$

The total change in spray area is thus a function of the area change of the mean-drop size D_{20}^2, and also the change in the total number of drops N_T due to the complete vaporization of the small drops in the spray.

Since $\overline{Nu} = Nu_{20}$ (±5 percent) (ref. 1), equation (5) may be written as

$$Nu_{20} = \frac{V_{20}}{\lambda} \frac{d\left(D_{20}^2\right)}{dx}\left[1 + \frac{d(\ln N_T)}{d\left(\ln D_{20}^2\right)}\right] \tag{6}$$

where V_{20} is the velocity of a drop in the spray having the same diameter as the mean drop size D_{20} and the Nusselt number is defined as $Nu_{20} = hD_{20}/k_g$.

The method of evaluating $d(\ln N_T)/d\left(\ln D_{20}^2\right)$ is given in appendix B. By substituting the value of this ratio into equation (6) and also the values of $d\left(D_{20}^2\right)/dx$ obtained from the plot of D_{20}^2 as a function of x (fig. 8), it was possible to calculate values of the Nusselt number Nu_{20}.

In reference 4 the following expression was derived for the Nusselt number of single drops:

$$Nu = 2 + 2.58\times10^6\left(\frac{Re\ Sc\ gl}{\overline{c}^2}\right)^{0.6}\left(\frac{k_g}{k_v}\right)^{0.5} \tag{7}$$

In order to obtain a similar correlation for sprays, the following temperature conditions were used to evaluate Nu_{20} and Re_{20}:

(1) At the liquid-film interface for the fine and the coarse sprays at T_s of 118° and 111° C, respectively, for both Nu_{20} and Re_{20}

(2) At the gas-film interface for the fine and the coarse sprays at T_g of 1381° and 1708° C, respectively, for both Nu_{20} and Re_{20}

(3) At the average film temperature for the fine and the coarse sprays at T_f of 750° and 910° C, respectively, for Nu_{20}; at the stoichiometric flame temperature for both the fine and the coarse sprays at 5000° F for Re_{20} (This procedure was also used in ref. 1.)

(4) At the average film temperature for the fine and the coarse sprays at T_f of 750° and 910° C, respectively for both Nu_{20} and Re_{20}

Film properties used in the fourth method of computation are given in table II, and properties of ethanol and the combustion gases are summarized in table III. The combustion temperature and gas properties were determined by a general method for automatic computation based on equilibrium composition of the combustion gases (ref. 5).

The results of these calculations are shown in figure 9, and it is evident that methods 1 and 2 do not agree with single-drop data (eq. (7)), whereas methods 3 and 4 do agree with equation (7) to within ±10 percent. Evaluation of both the Nusselt and the Reynolds numbers at the average film temperature (method 4) may be preferable since the combustion-gas temperature is treated as a function of the oxidant-fuel ratio. Vaporization tests made at near-stoichiometric mixtures in a combustor would aid in making a choice between these two methods. Since the data agree well with equation (7), the chamber-pressure fluctuations appeared to have little effect on the heat-transfer Nusselt numbers for the conditions of this investigation.

Momentum-Transfer Relations

According to Newton's second law of motion, the force F on a vaporizing drop may be equated to the change of momentum of the drop with time to give the following expression for the case of varying mass and velocity:

$$F = \frac{d(mV)}{dt} = m\frac{dV}{dt} + V\frac{dm}{dt} \tag{8}$$

Equating the instantaneous force F on the drop to the aerodynamic pressure force of the combustion-gas stream yields the following expression:

$$\frac{d(mV_l)}{dt} = \frac{1}{2}\rho_g A_d (V_g - V_l)^2 C_D \tag{9}$$

where C_D is the droplet drag coefficient.

For the case of a spray of drops, equation (9) may be rewritten as

$$\frac{d\sum_{D=0}^{D=D_m} nD^3 V_l}{dt} = \frac{3}{4}\frac{\rho_g}{\rho_l}\sum_{D=0}^{D=D_m} nD^2(\Delta V)^2 C_D \tag{10}$$

since $\Delta V = V_g - V_l$ and $A_d = \pi D^2/4$. In order to simplify equation (10), the following expressions were derived:

$$V_{30} = \frac{\sum_{D=0}^{D=D_m} nD^3 V_l}{\sum_{D=0}^{D=D_m} nD^3}$$

and

$$(C_D)_{20}(\Delta V)_{20}^2 = \frac{\sum_{D=0}^{D=D_m} nD^2(\Delta V)^2 C_D}{\sum_{D=0}^{D=D_m} nD^2}$$

From the experimental drop-size (table I) and the drop-velocity (fig. 6) data and the drag-coefficient expressions (ref. 1), these expressions were evaluated and found to be accurate to within ±5 percent. Equation (10) may be thus simplified as follows:

$$\frac{d\left(V_{30} N_T D_{30}^3\right)}{dt} = \frac{3}{4} \frac{\rho_g}{\rho_l} N_T D_{20}^2 (\Delta V)_{20}^2 (C_D)_{20} \qquad (11)$$

since

$$\sum_{D=0}^{D=D_m} nD^3 = N_T D_{30}^3$$

and

$$\sum_{D=0}^{D=D_m} nD^2 = N_T D_{20}^2$$

Taking the derivative of the left side of equation (11) according to equation (8) gives

$$\frac{d\left(V_{30}N_T D_{30}^3\right)}{dt} = N_T D_{30}^3 \frac{dV_{30}}{dt} + V_{30} \frac{d\left(N_T D_{30}^3\right)}{dt} \tag{12}$$

Equation (12) may be rewritten as

$$\frac{d\left(V_{30}N_T D_{30}^3\right)}{dt} = V_{30}N_T \frac{dD_{30}^3}{dt}\left[1 + \frac{d(\ln N_T)}{d\left(\ln D_{30}^3\right)} + \frac{d(\ln V_{30})}{d\left(\ln D_{30}^3\right)}\right] \tag{13}$$

Substituting it into equation (11) gives the following expression for the drag coefficient:

$$(C_D)_{20} = \frac{4}{3}\frac{\rho_l}{\rho_g}\frac{V_{30}^2}{(\Delta V)_{20}^2}\left(\frac{dD_{30}^3}{dx}\right) D_{20}^{-2}\left[1 + \frac{d(\ln N_T)}{d\left(\ln D_{30}^3\right)} + \frac{d(\ln V_{30})}{d\left(\ln D_{30}^3\right)}\right] \tag{14}$$

where V_{30} is the velocity of a drop in a spray with $D = D_{30}$ and $(\Delta V)_{20} = V_g - V_{20}$ and V_{20} is the velocity of a drop in a spray with $D = D_{20}$. Values of N_T at each x-distance were determined by the method described in appendix B, and corresponding values of D_{30} were obtained from the drop-size-distribution data. Values of V_{20} and V_{30} were obtained from figure 6 for drops with diameters $D = D_{20}$ and $D = D_{30}$, respectively.

The relation between V_{30} and D_{30}^3 was determined from the slope of the curves in figure 10 and the relation between N_T and D_{30}^3 from the slope of the curve in figure 11. By substituting these values and the slope dD_{30}^3/dx obtained from figure 12 into equation (14), it was possible to calculate drag coefficients for the mean-drop size D_{20}.

In reference 1, the following expression was derived:

$$(C_D)_{20} = 0.13\ Re_{20}^{-0.84}\left(\frac{gl}{\bar{c}^2}\right)^{-0.2} \tag{15}$$

Therefore, the drag coefficients determined from equation (14) for two film-temperature conditions were plotted as functions of the product $Re_{20}^{-0.84}(gl/\bar{c}^2)^{-0.2}$ (fig. 13). Drag-coefficient data obtained in reference 1 are also included for comparison, and agreement of ±10 percent with equation (15) is shown. Thus, the presence of chamber-pressure fluctuations did not show any appreciable effect on drag coefficients obtained in this investigation (fig. 13).

Combustor-Performance Calculations

To determine the performance of the combustor, the characteristic exhaust velocity c^* was calculated from the expression

$$c^* = P_c g \frac{A_t}{W_t} \tag{16}$$

where A_t is the area of the nozzle throat, 0.857 square inch, and $W_T = W_p + W_{N_2} = 0.395$ and 0.370 pound per second for chamber pressures of 57.0 and 48.5 pounds per square inch absolute, respectively. Nitrogen-gas flow rates were 0.097 and 0.072 pound per second for the fine and the coarse sprays, respectively. Results from this study are given in table IV in which values of c^*_{theor} were calculated by the method given in reference 4.

The volume percent of the fuel vaporized E was determined from the expression

$$E = \left[1 - \frac{\left(N_T D_{30}^3\right)_f}{\left(N_T D_{30}^3\right)_i} \right] \times 100 \tag{17}$$

where the product $N_T D_{30}^3$ was evaluated at each downstream distance x by referring to figures 11 and 12. Values of E are plotted as functions of the downstream distance x (fig. 14), and the total volume percent of fuel vaporized for each of the two test conditions is given in table IV.

On a theoretical basis, the percent by volume of fuel vaporized may be assumed approximately equal to the combustion efficiency, which is proportional to the absolute temperature of the combustion gases T_g. Theoretical rocket-performance calculations show that $c^*/c^*_{theor} \sim \sqrt{T_g}$. Thus, theory predicts that

$$E = \left(\frac{c^*}{c^*_{theor}} \right)^2$$

Experimental results given in table IV show an agreement with theory of ±2 percent.

SUMMARY OF RESULTS

Fuel-spray vaporization-rate equations, derived for relatively steady-state combustion, may be applied in the case of low-frequency chamber-pressure fluctuations (for random amplitude variations as high as 37 percent of the average chamber pressure) without modifying the expressions; that is, the heat-transfer and drag coefficients based on the average chamber pressure and the area-mean drop diameter were within ±10 percent of the values calculated for steady-state combustion. Also, analysis of the combustion data showed that the completeness of vaporization of the fuel spray in the combustor was equal to the square of the characteristic-exhaust-velocity efficiency, with an agreement of ±2 percent.

Lewis Research Center
National Aeronautics and Space Administration
Cleveland, Ohio, July 6, 1962

APPENDIX A

SYMBOLS

A	area, sq cm or sq ft
$b_{g,w}$	molecular mass diffusivity evaluated at T_f, g/(cm)(sec)
C_D	drag coefficient
$\bar{c}$	root-mean-square velocity of gas molecules, cm/sec
c_p	specific heat at constant pressure, g-cal/(g)($^{\circ}$C)
c^*	characteristic exhaust velocity, ft/sec
c^*_{theor}	theoretical characteristic exhaust velocity, ft/sec
D	drop diameter, microns
D_{20}	area-mean diameter defined by general expression: $(D_{e,f})^{e-f} = \sum nD^e / \sum nD^f$ which gives $D_{20} = \left(\sum nD^2 / \sum n\right)^{1/2}$, microns
D_{30}	volume-mean drop diameter, $\left(\sum nD^3 / \sum n\right)^{1/3}$, microns
dm/dt	vaporization rate, g/sec
dQ/dt	heat-transfer rate
E	volume of fuel vaporized, percent
e	mean-diameter notation
F	force on a vaporizing drop, g-cm/sec^2
f	mean-diameter notation
g	acceleration due to gravity, 980 cm/sec^2
H_T	total heat required per unit mass to increase temperature from T_l to T_y, g-cal/g

H_v latent heat of vaporization, g-cal/g

h heat-transfer coefficient, g-cal/(sec)(cm^2)(^oC)

k thermal conductivity, (g-cal)(cm)/(sec)(cm^2)(^oC)

l mean free path of air molecules, cm

M molecular weight

m mass of liquid, g

N_T total number of drops in a spray

Nu heat-transfer Nusselt number for a single drop, hD/k_g

$\overline{Nu}$ average heat-transfer Nusselt number, $h\overline{D}/k_g$

Nu_{20} heat-transfer Nusselt number for drop of diameter $D = D_{20}$, hD_{20}/k_g

n number of drops in given size range

P_c chamber pressure, lb/sq in. abs

Q heat requirement, g-cal

Re Reynolds number of single drop, $D\ \Delta V\rho_g/\mu_g$

Re_{20} Reynolds number based on drop of diameter $D = D_{20}$, $D_{20}\ \Delta V\rho_g/\mu_g$

Sc Schmidt number, $\mu_g/b_{g,w}$

T temperature, ^oC

ΔT difference between gas temperature and surface temperature of drop, $T_g - T_s$, ^oC

T_f average film temperature, $(T_g + T_s)/2$, ^oC

t time, sec

V velocity, ft/sec

ΔV relative velocity of combustion gas with respect to drop, cm/sec

V_{20} velocity of a drop in spray having diameter $D = D_{20}$, ft/sec

W	total weight flow, lb/sec
x	distance downstream from injector face, in. or ft
λ	evaporation constant, $4k_g \Delta t/\rho_l H_T$, cm^2/sec
μ	viscosity, poises
ρ	density, g/cc
σ	molecular diameter, cm

Subscripts:

c	completely evaporated
d	drop
f	film or final
g	combustion gas
i	initial
l	liquid
m	maximum
N_2	nitrogen gas
p	propellants
s	surface
stoic	stoichiometric
T	total
t	nozzle throat
v	vapor or volume
y	condition for evaluating temperature
20	based on mean drop diameter, D_{20}
30	based on mean drop diameter, D_{30}

APPENDIX B

EVALUATION OF $d(\ln N_T)/d\left(\ln D_{20}^2\right)$

The diameter of a drop that is just completely evaporated D_c in an incremental distance Δx may be calculated from the expression

$$D_c^2 = \lambda \overline{Nu}\left(\frac{\Delta x}{\overline{V}_l}\right)$$

where the average Nusselt number $\overline{Nu}$ is based on the average Reynolds number $\overline{Re} = \overline{D}(\overline{V}_g - \overline{V}_l)\rho_g/\mu_g$, as given in the relation

$$\overline{Nu} = 2 + 2.58\times10^6\ \overline{Re}\left(\frac{g_l}{\overline{c}^2}\right)^{0.6}\left(\frac{k_g}{k_v}\right)^{0.5}$$

In the definition of $\overline{Re}$, $\overline{D} = D_c/2$, $\overline{V}_l$ is the average drop velocity over the distance Δx, and $\overline{V}_g$ is the average gas velocity over the same distance.

By means of the following trial-and-error method, the complete vaporization of small drops from stations x of 6 to 10 inches may be determined. If it is assumed that $D_c \simeq 60$ microns, then $\overline{D} \simeq 30$ microns. Since at $\overline{x} = 8$ inches $\overline{V}_g = 268$ feet per second and $\overline{V}_l = 145$ feet per second, $\overline{\Delta V} = 123$ feet per second. Therefore, $\overline{Re} = 18.9$, $\overline{Nu} = 2.91$, $D_c = 49.6$ microns. The assumption that $D_c \simeq 60$ microns was too high and the calculation is repeated for $D_c \simeq 40$ microns, which results in $D_c = 46$ microns. Finally, it is assumed that $D_c \simeq 50$ microns, which yields $D_c \simeq 48$ microns. Therefore, $D_c = 49$ microns is taken as the final value.

From the drop-size distribution data at $x = 6$ inches, a plot of $\sum_{D=0}^{D=D} n \Big/ \sum_{D=0}^{D=D_m} n$ as a function of D was obtained (fig. 15). For this condition $D = D_c = 49$ microns and the fractional number of drops in the spray that are completely vaporized is 0.10. Also, since

$$\Delta N_T = N_T \frac{\sum_{D=0}^{D=D_c} n}{N_T} = 516(0.10) = 52 \text{ drops}$$

Then at $x = 10$ inches

$$(N_T)_f = (N_T)_i - \Delta N_T = 516 - 52 = 464 \text{ drops}$$

The same method of calculation is repeated to determine N_T at $x = 15$ inches. The values of N_T are plotted against values of D_{20}^2, obtained at the same station x, as shown in figure 16. From this plot, it is evident that

$$\frac{d(\ln N_T)}{d\left(\ln D_{20}^2\right)} = 0.45 \pm 0.02,$$

which agrees within ±5 percent of the evaluation made in reference 1.

REFERENCES

1. Ingebo, R. D.: Heat-Transfer and Drag Coefficients for Ethanol Drops in a Rocket Chamber Burning Ethanol and Liquid Oxygen. Eighth Symposium (International) on Combustion, The Williams & Wilkins Co., 1962, pp. 1104-1113.

2. Priem, Richard J., and Heidmann, Marcus F.: Vaporization of Propellants in Rocket Engines. ARS Jour., vol. 29, no. 11, Nov. 1959, pp. 836-842.

3. Ingebo, Robert D.: Photomicrographic Tracking of Ethanol Drops in a Rocket Chamber Burning Ethanol and Liquid Oxygen. NASA TN D-290, 1960.

4. Ingebo, Robert D.: Study of Pressure Effects on Vaporization Rate of Drops in Gas Streams. NACA TN 2850, 1953.

5. Gordon, Sanford, Zeleznik, Frank J., and Huff, Vearl N.: A General Method for Automatic Computation of Equilibrium Compositions and Theoretical Rocket Performance of Propellants. NASA TN D-132, 1959.

TABLE I. - DROP-SIZE-DISTRIBUTION DATA

Fine spray						Coarse spray					
Downstream distance, x, in.											
6		10		15		6		10		15	
Average drop diameter, D, microns (a)	Number of drops in given drop-size increment, n	Average drop diameter, D, microns (b)	Number of drops in given drop-size increment, n	Average drop diameter, D, microns (b)	Number of drops in given drop-size increment, n	Average drop diameter, D, microns (c)	Number of drops in given drop-size increment, n	Average drop diameter, D, microns (d)	Number of drops in given drop size increment, n	Average drop diameter, D, microns (d)	Number of drops in given drop-size increment, n
16	21	11	69	11	140	32	98	27	281	27	370
43	40	28	66	28	156	86	137	72	282	72	317
64	44	43	77	43	162	129	111	107	144	107	169
86	57	57	101	57	138	172	62	143	114	143	104
107	54	71	108	71	123	215	38	179	86	179	83
129	48	85	123	85	111	258	22	214	68	214	74
150	40	100	99	100	115	301	17	250	48	250	53
172	26	114	81	114	97	344	12	286	34	286	31
193	16	128	63	128	81	387	8	321	22	321	23
215	8	143	61	143	69	430	5	357	13	357	10
236	6	157	48	157	48	473	3	393	7	393	7
258	5	171	36	171	26	516	2	428	5	428	3
279	3	185	25	185	17	559	1	464	3	464	1
301	1	200	18	200	11	---	---	500	2	---	---
322	1	214	15	214	7	---	---	535	2	---	---
---	---	228	10	228	3	---	---	---	---	---	---
---	---	243	6	---	---	---	---	---	---	---	---
---	---	257	4	---	---	---	---	---	---	---	---
---	---	271	3	---	---	---	---	---	---	---	---
---	---	285	1	---	---	---	---	---	---	---	---

[a]Initial increment, 31.5 microns; remaining increments, 21.5 microns.

[b]Initial increment, 21 microns; remaining increments, 14 microns.

[c]Initial increment, 64 microns; remaining increments, 43 microns.

[d]Initial increment, 54 microns; remaining increments, 36 microns.

TABLE II. - FILM PROPERTIES EVALUATED AT AVERAGE FILM TEMPERATURE

Fuel spray	Chamber pressure, P_c, atm	Gas viscosity, μ_g, poises	Molecular mass diffusivity, $b_{g,w}$, g/(cm)(sec)	Schmidt number, Sc	Molecular diameter, σ, cm	Molecular weight of combustion gas, M_g	$gl/\overline{c}^2$	Thermal conductivity of combustion gas, k_g, cal/(sec)(°C)(cm)	Thermal conductivity of vapor, k_v, cal/(sec)(°C)(cm)
Fine	3.88	3.40×10^{4}	4.17×10^{4}	0.89	2.95×10^{8}	18.85	6.78×10^{13}	3.0×10^{4}	1.8×10^{4}
Coarse	3.30	3.90	4.48	.87	2.95	19.27	8.15	3.2	2.3

TABLE III. - FUEL AND COMBUSTION-GAS PROPERTIES

Fuel spray	Chamber pressure, P_c, atm	Injection temperature, T_l, °C	Surface temperature, T_s, °C	Average film temperature, T_f, °C	Combustion gas temperature, T_g, °C	Fluid density of liquid, ρ_l, g/cc	Fluid density of combustion gas, ρ_g, g/cc	Latent heat of evaporation, H_v, cal/g	Specific heat of liquid at constant pressure, $c_{p,l}$, cal/(g)(°C)	Specific heat of vapor at constant pressure, $c_{p,v}$, cal/(g)(°C)	Evaporation constant at T_f, λ, cm^2/sec
Fine	3.88	22	118	750	1381	0.68	8.72×10^{4}	187	0.68	0.58	33.8×10^{-4}
Coarse	3.30	22	111	910	1708	.68	6.56	190	.68	.60	36.8

TABLE IV. - COMBUSTION AND VAPORIZATION RESULTS

Fuel spray	Average chamber pressure, lb/sq in. abs	Amplitude of fluctuation, $(\Delta P_c/P_c) \times 100$, percent	Characteristic exhaust velocity, c^*, ft/sec	Characteristic-exhaust-velocity efficiency, percent	Percent by volume of fuel vaporized, E, volume percent
Fine	57.0	37	3980	98	94
Coarse	48.5	10	3620	88	78

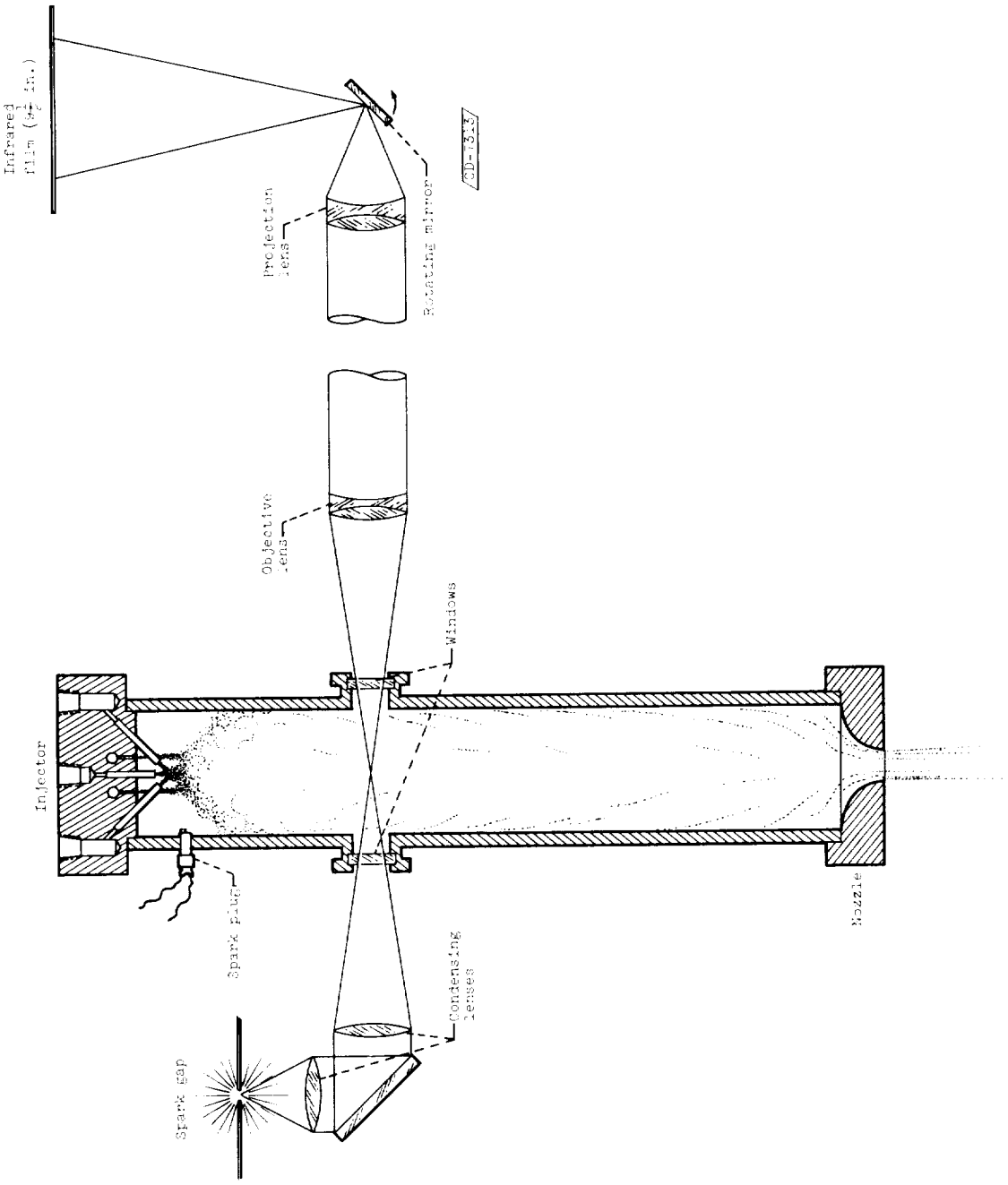

Figure 1. - Diagram of experimental apparatus.

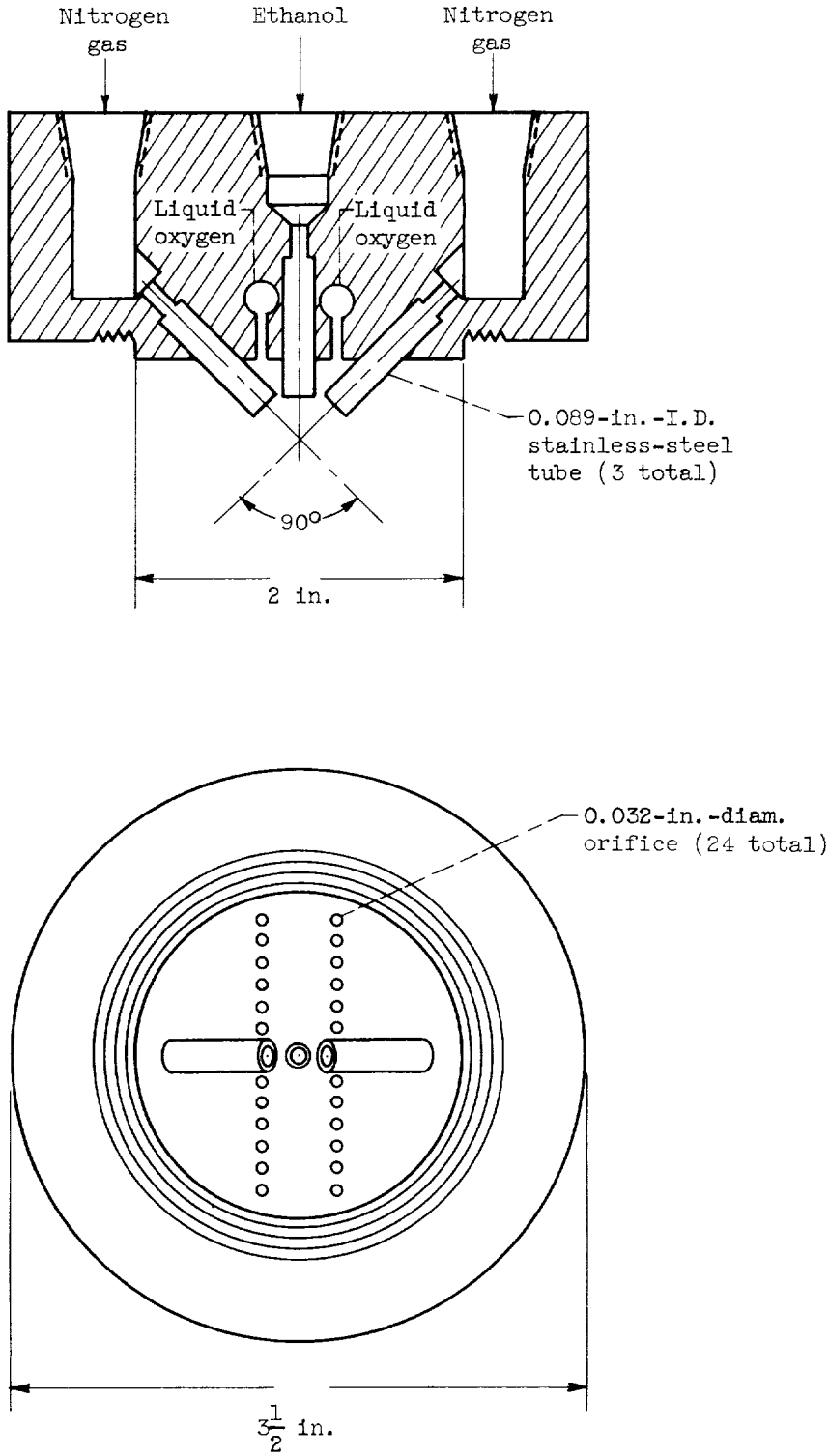

Figure 2. - Detail of propellant injector.

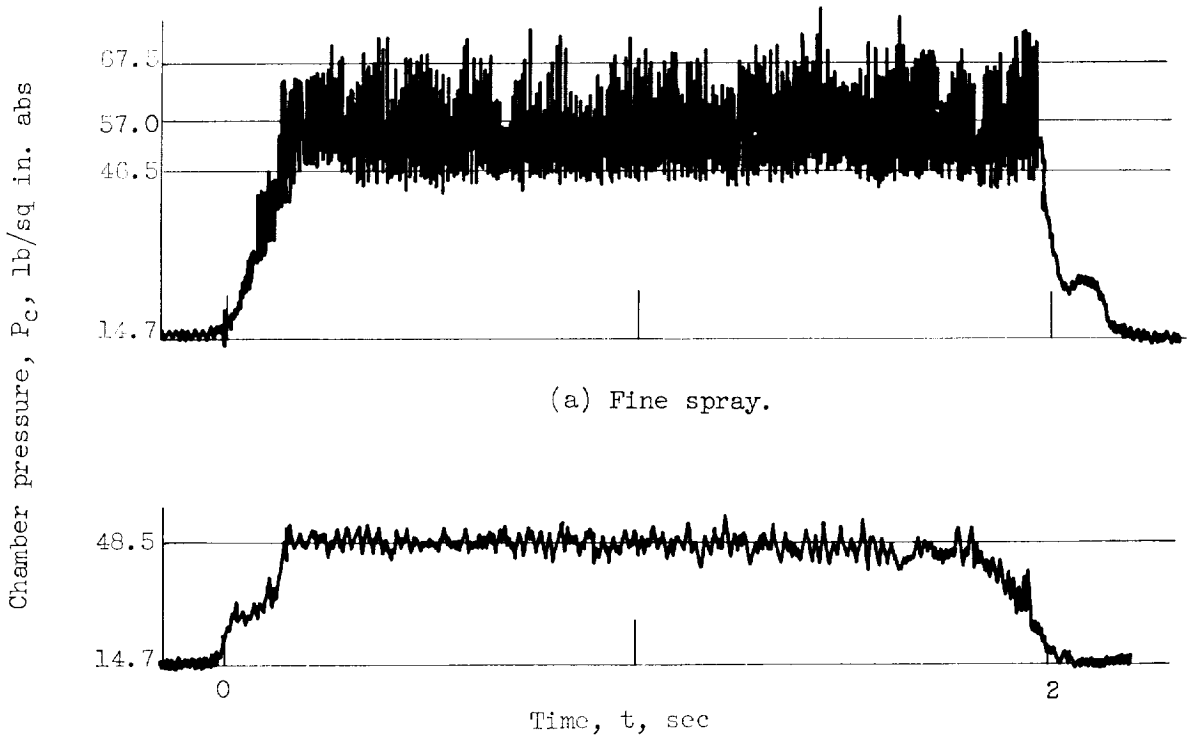

(a) Fine spray.

(b) Coarse spray.

Figure 3. - Chamber-pressure fluctuations.

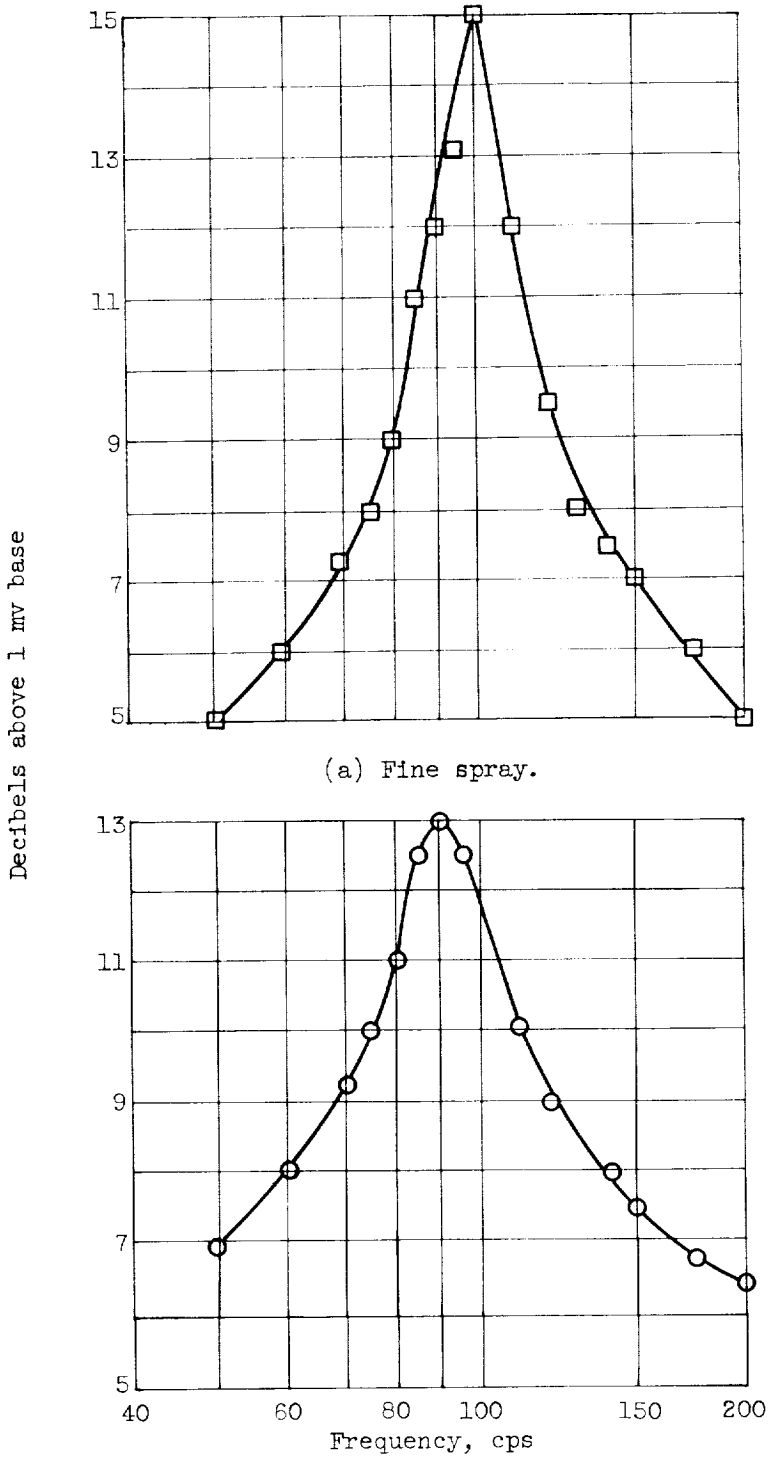

(a) Fine spray.

(b) Coarse spray.

Figure 4. - Frequency spectrum of chamber-pressure fluctuations.

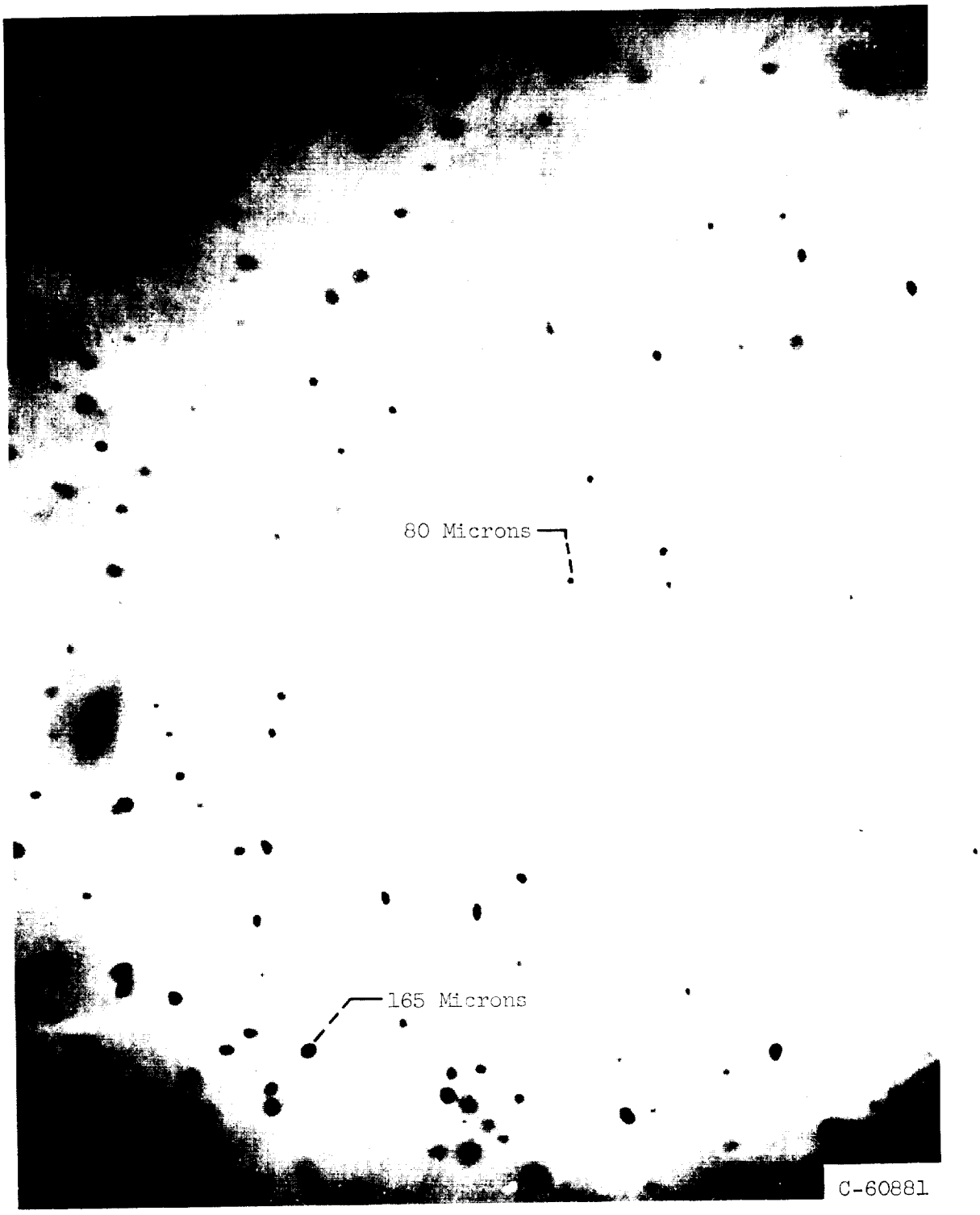

Figure 5. - Photomicrograph of fine spray taken 10 inches downstream from injector face. ×14.

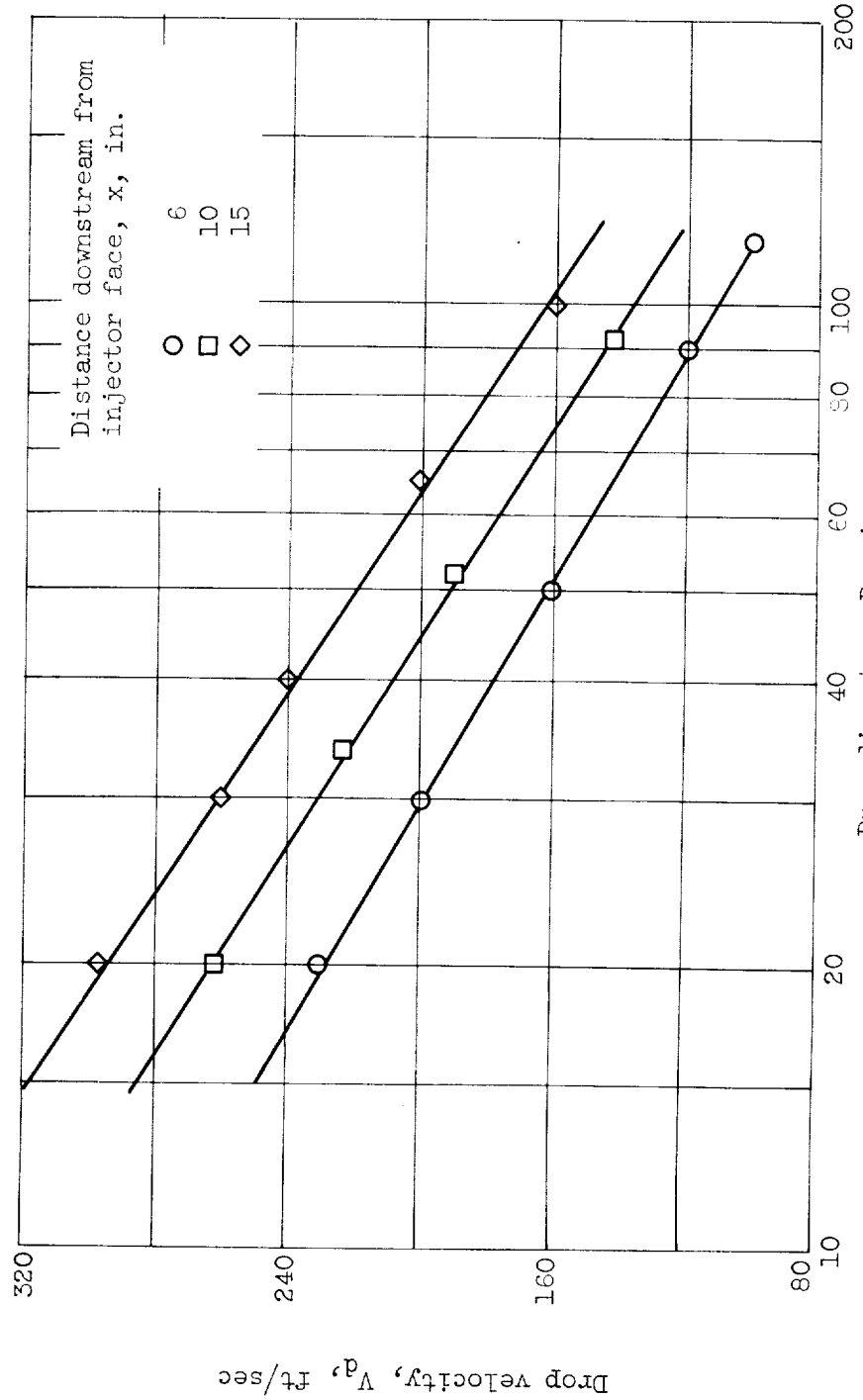

(a) Fine spray.

Figure 6. - Drop-size and drop-velocity data.

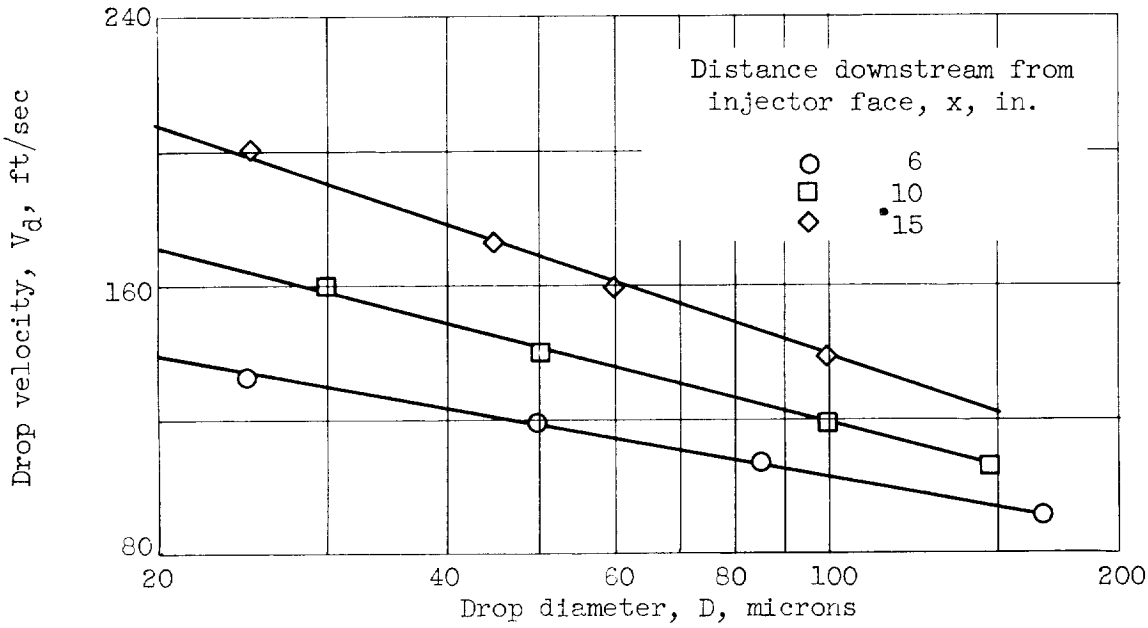

(b) Coarse spray.

Figure 6. - Concluded. Drop-size and drop-velocity data.

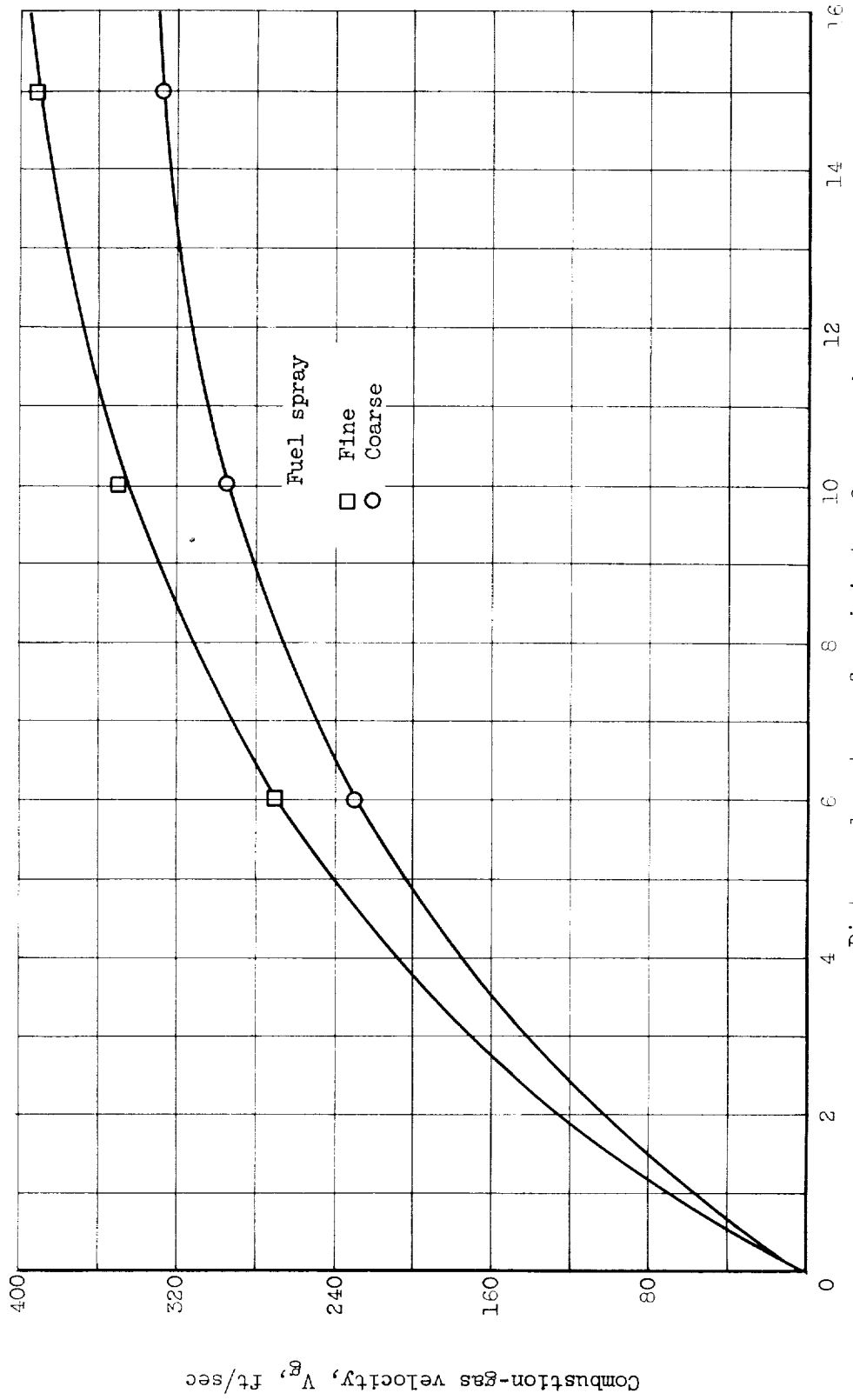

Figure 7. - Combustion-gas velocity in 16-inch-long chamber.

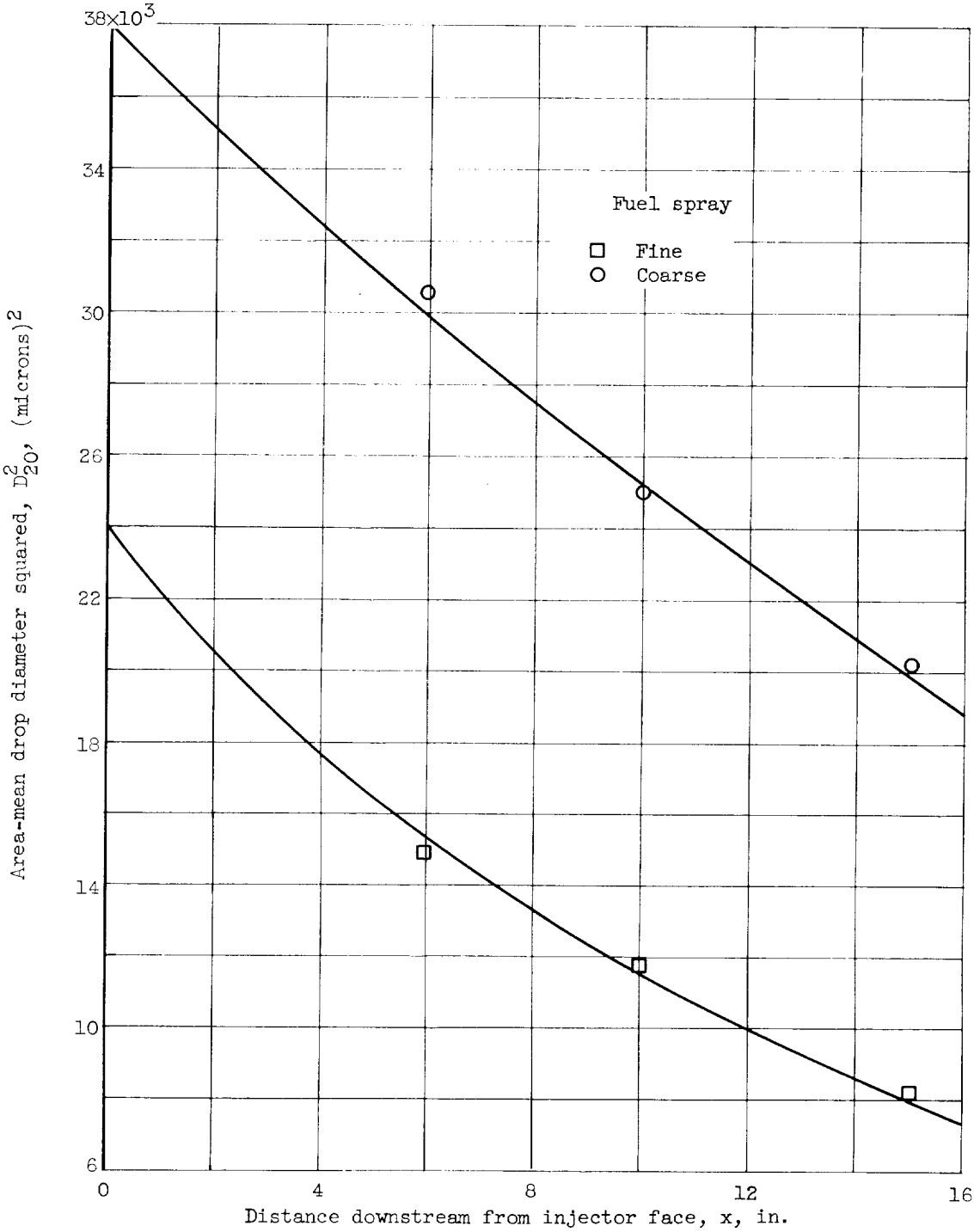

Figure 8. - Evaporation of ethanol spray represented by area-mean drop diameter.

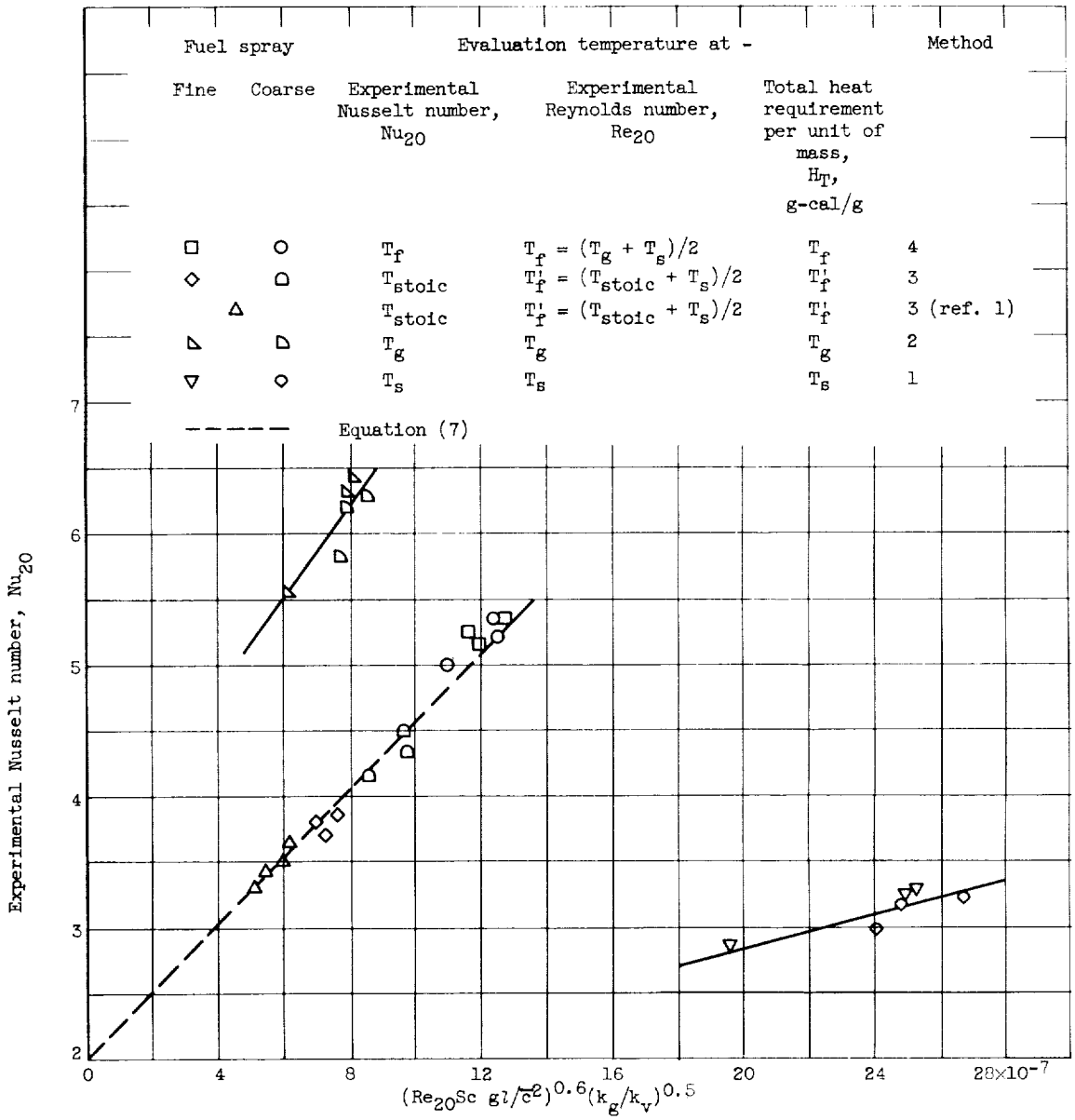

Figure 9. - Correlation of experimental Nusselt number with equation (7).

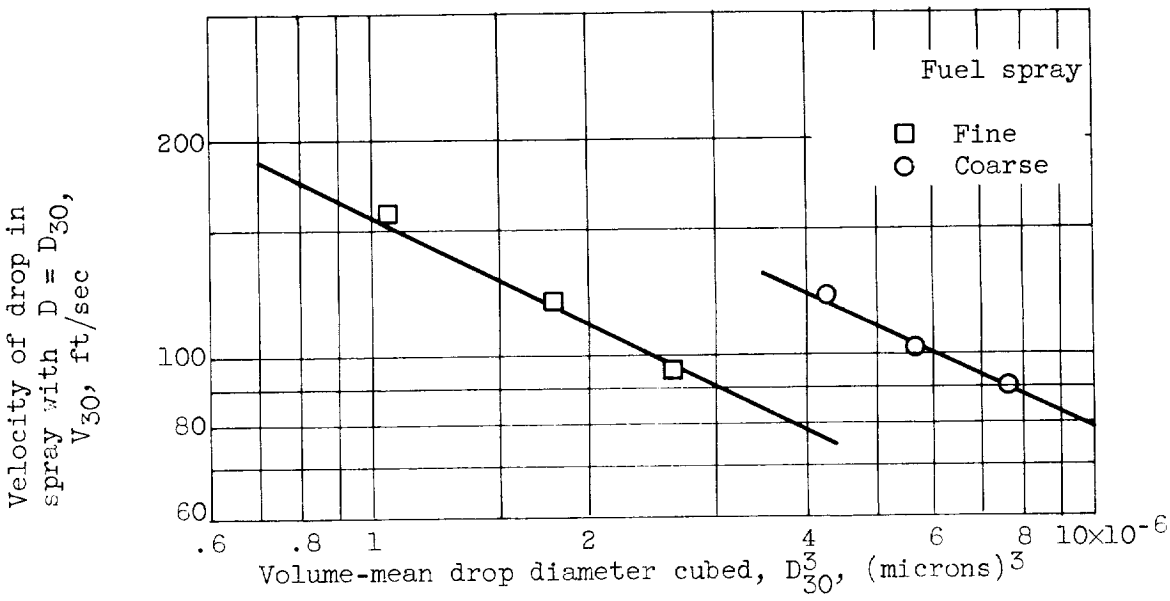

Figure 10. - Relation between velocity and diameter of mean drop size.

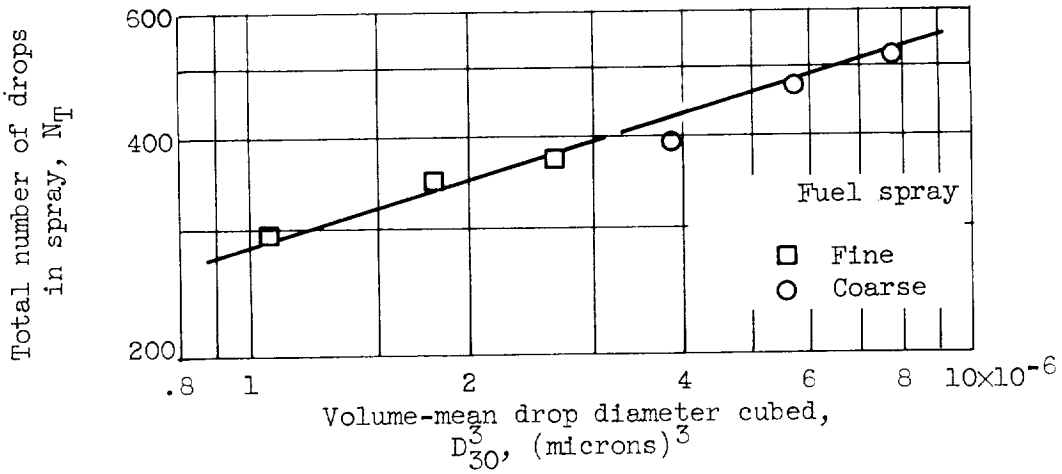

Figure 11. - Relation between total number of drops in spray and mean-diameter.

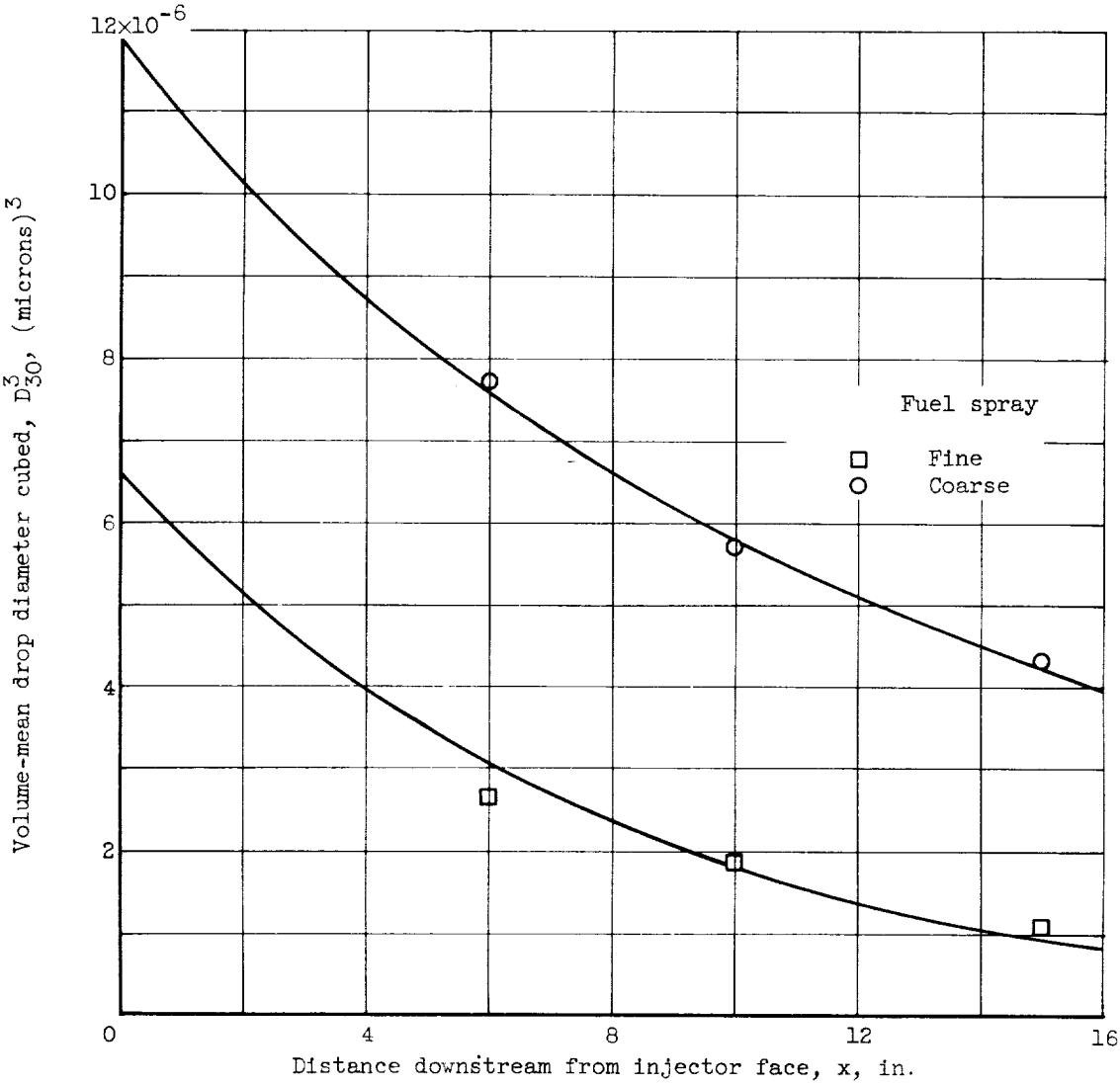

Figure 12. - Vaporization rate of volume-number mean drop diameter.

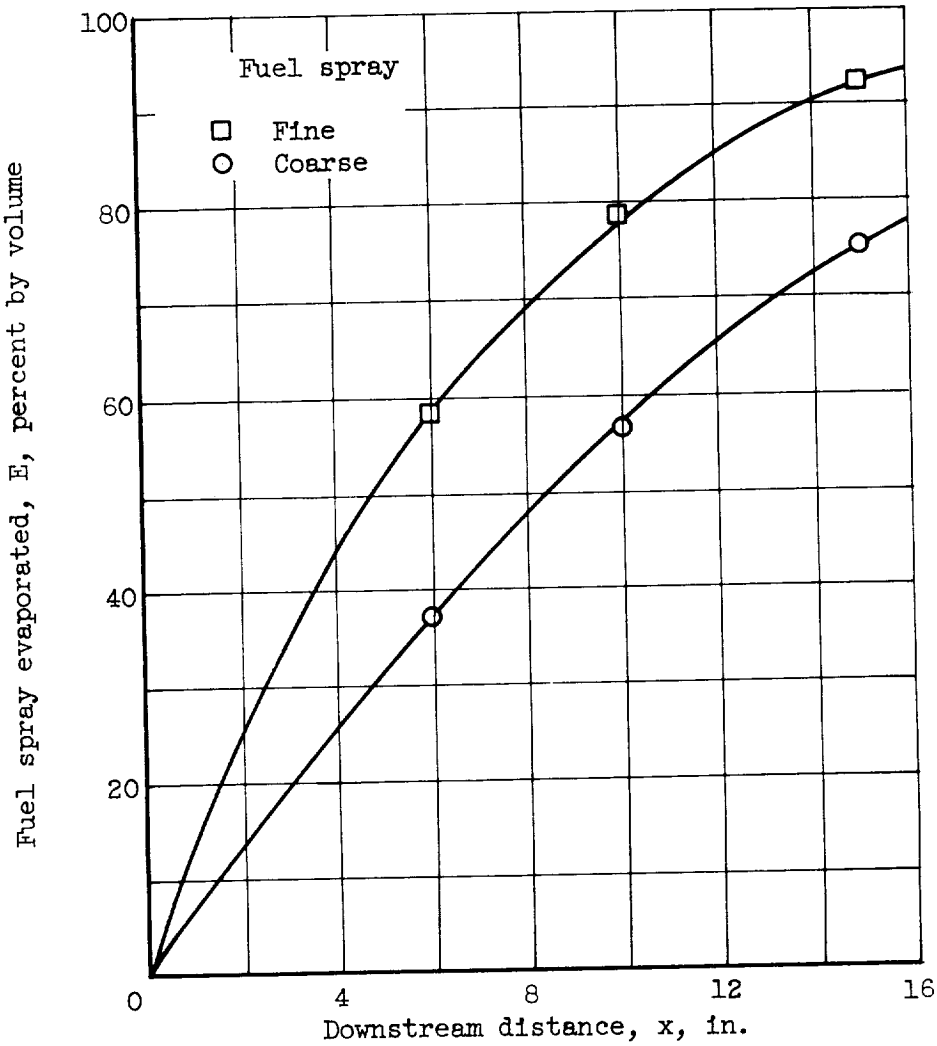

Figure 14. - Volume of fuel spray evaporated in rocket combustor.

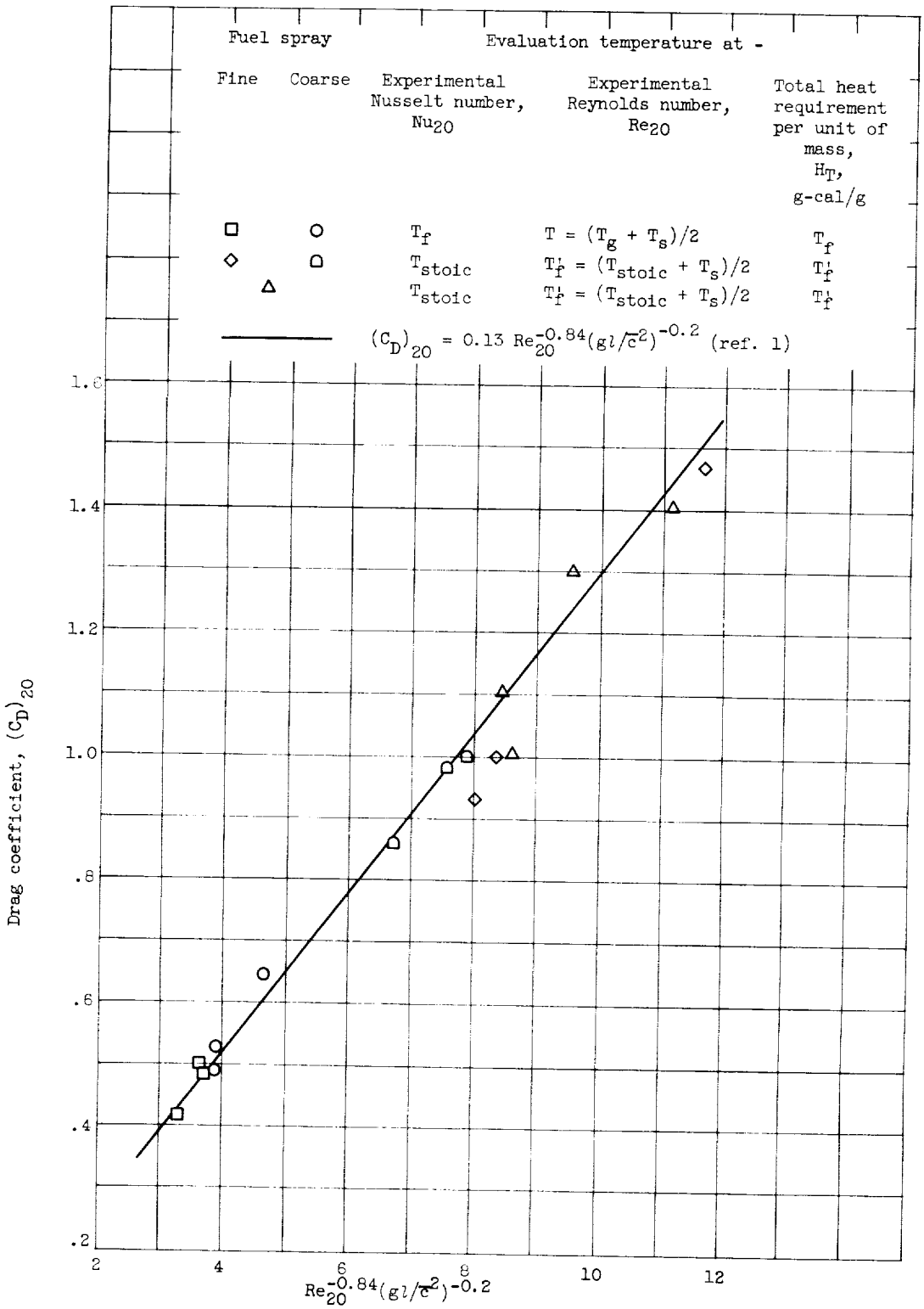

Figure 13. - Correlation of drag coefficient with Reynolds number and $gl/\bar{c}^2$ group.

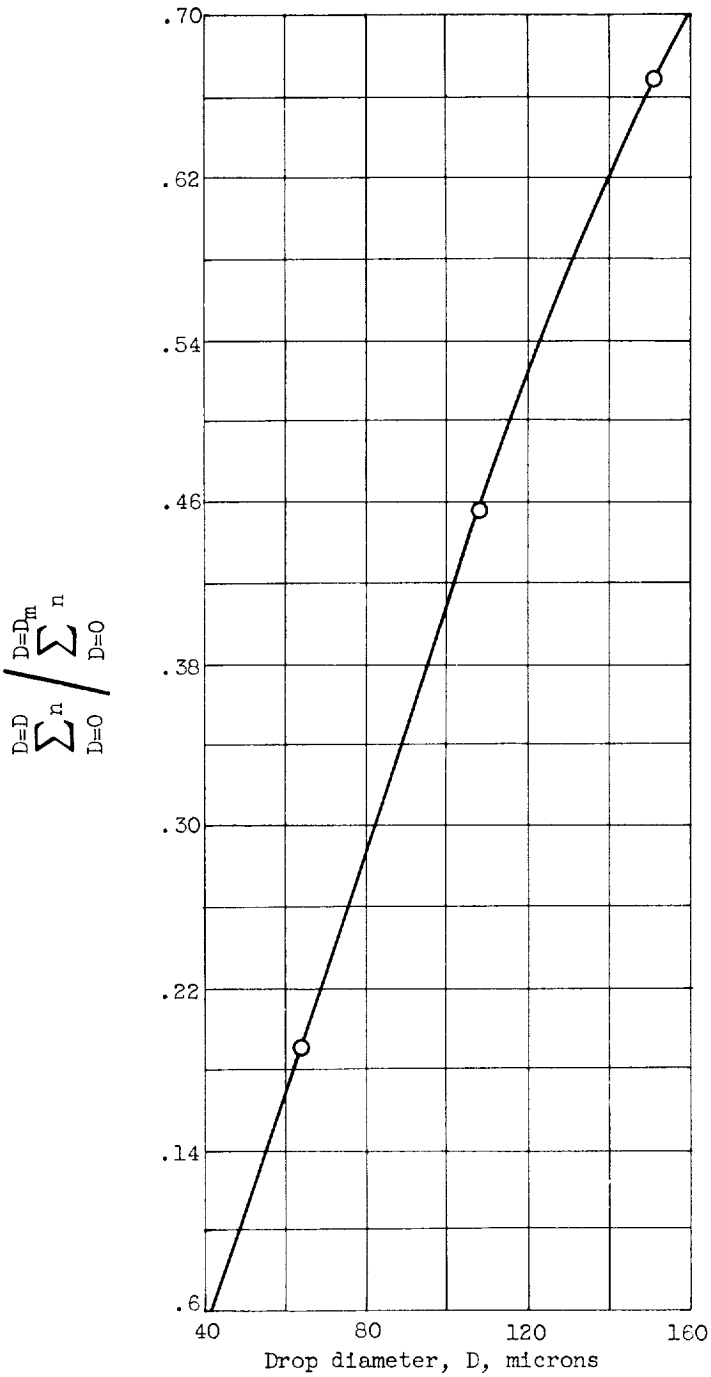

Figure 15. - Relation between $\sum_{D=0}^{D=D} n \Big/ \sum_{D=D}^{D=D_m} n$ and drop diameter for coarse spray; distance downstream from injector face, 6 inches.

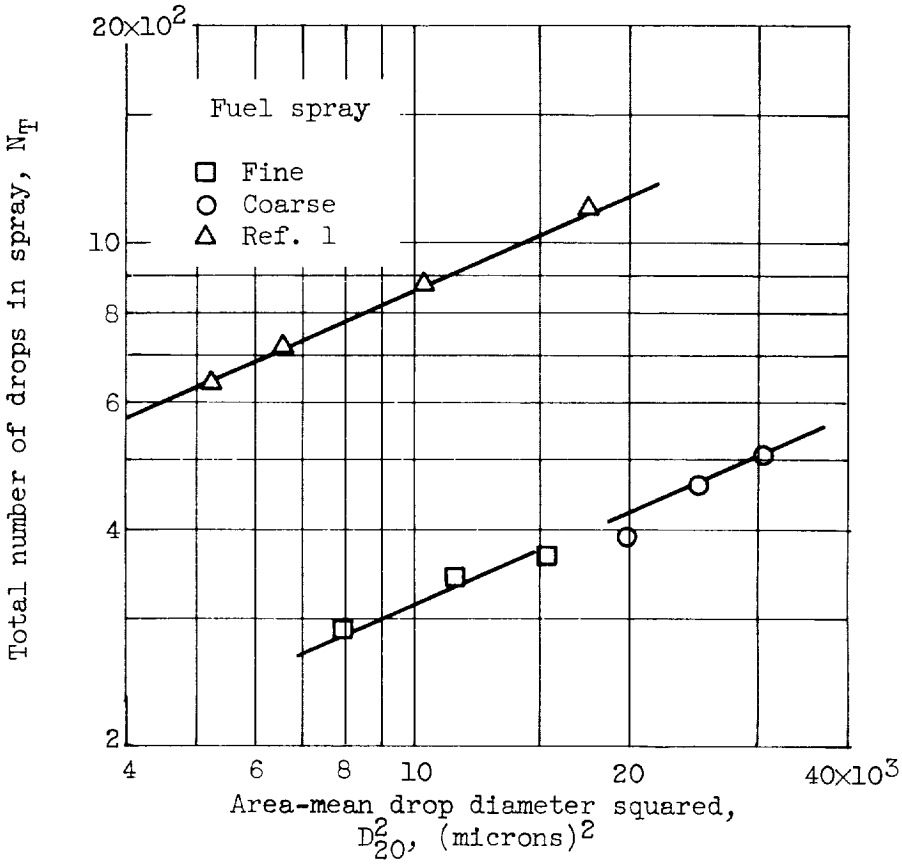

Figure 16. - Relation between total number of drops in spray and area-mean drop diameter squared.